Direct, high-throughput linking of single-cell imaging and gene expression

Catherine K Xu[1,2]*, Georg Meisl[3], Nikita Moshkov[4], Niklas A Schmacke[4], Karolis Goda[5], Alexey Shkarin[1], Maximilian F Schlögel[1], Tuomas PJ Knowles[3,6], Fabian J Theis[4,7,8], Linas Mazutis[5], Jochen Guck[1,2]†

To whom correspondence should be addressed: cathxu@ethz.ch

†Deceased

[1]Max Planck Institute for the Science of Light, Erlangen, Germany

[2]Max Planck Zentrum für Physik und Medizin, Erlangen, Germany

[3]Yusuf Hamied Department of Chemistry, University of Cambridge, Cambridge, UK

[4]Institute of Computational Biology, Helmholtz Munich, Munich, Germany

[5]Institute of Biotechnology, Vilnius University, Vilnius, Lithuania

[6]Cavendish Laboratory, University of Cambridge, Cambridge, UK

[7]TUM School of Life Sciences Weihenstephan, Technical University of Munich, Munich, Germany

[8]School of Computation, Information and Technology, Technical University of Munich, Munich, Germany

Abstract

Single-cell technologies have transformed our ability to dissect cellular heterogeneity based on molecular composition. However, physical properties of live cells, such as size, morphology, and mechanical state, remain largely disconnected from molecular profiling, limiting our understanding of their relationship. We introduce im-seq, a high-throughput single-cell platform integrating live-cell imaging with mRNA sequencing, through multimodal barcoding, and demonstrate its application to haematopoietic cell lines.

Main text

In recent years the study of biological systems has been revolutionised by the development of single-cell technologies that enable the detailed characterisation of cellular heterogeneity [1, 2]. More recently, the emergence of multimodal single-cell approaches has demonstrated the importance of high-dimensional, information-rich data for dissecting complex biological processes [3]. In contrast, the dimension of optical characterisation is almost entirely lacking in this space, despite being the primary technology to investigate cell biology [4].

Existing methods to link live optical characterisation with transcriptomic readouts at the single-cell level are limited in throughput. Static, array-based approaches are inherently limited in throughput and do not scale easily, with existing technologies involving positional barcoding on arrays [5] or optical decoding of barcode bead sequences [6, 7, 8, 9, 10]. Deterministic flow-based systems which precisely control individual cells are more scalable, but reliance on high-precision handling ultimately limits their analysis rate [11, 12, 13]. While spatial transcriptomic methods can be higher in throughput, they require fixation, which renders phenotypes such as mechanical stiffness and secretion inaccessible [14, 15, 16].

To overcome these limitations, we developed a high-throughput, scalable, flow-based platform that integrates live-cell imaging, droplet-based scRNA-seq, and multimodal barcode decoding. Rather than enforcing determinism, we deliberately harness randomness to generate and decode combinatorial, multimodal barcodes on the fly. This approach thereby combines the versatility of imaging-based characterisation with the scalability of droplet sequencing workflows. Such multimodal single-cell technology will be invaluable for initiatives building virtual cell models in silico, providing both insights into inter-modality relationships and foundations for integrating single-modality datasets [17].

In droplet-based scRNA-seq, single cells are co-encapsulated with uniquely barcoded beads which index sequences during reverse transcription [18, 19, 20]. However, because these DNA barcodes are randomly distributed across optically identical beads (here referred to as blind barcode beads), we cannot associate optical data with the mRNA sequencing output. To overcome this, im-seq introduces an additional multimodal barcode into each droplet: a combinatorial tag that can be identified by both imaging and sequencing (Figure 1).

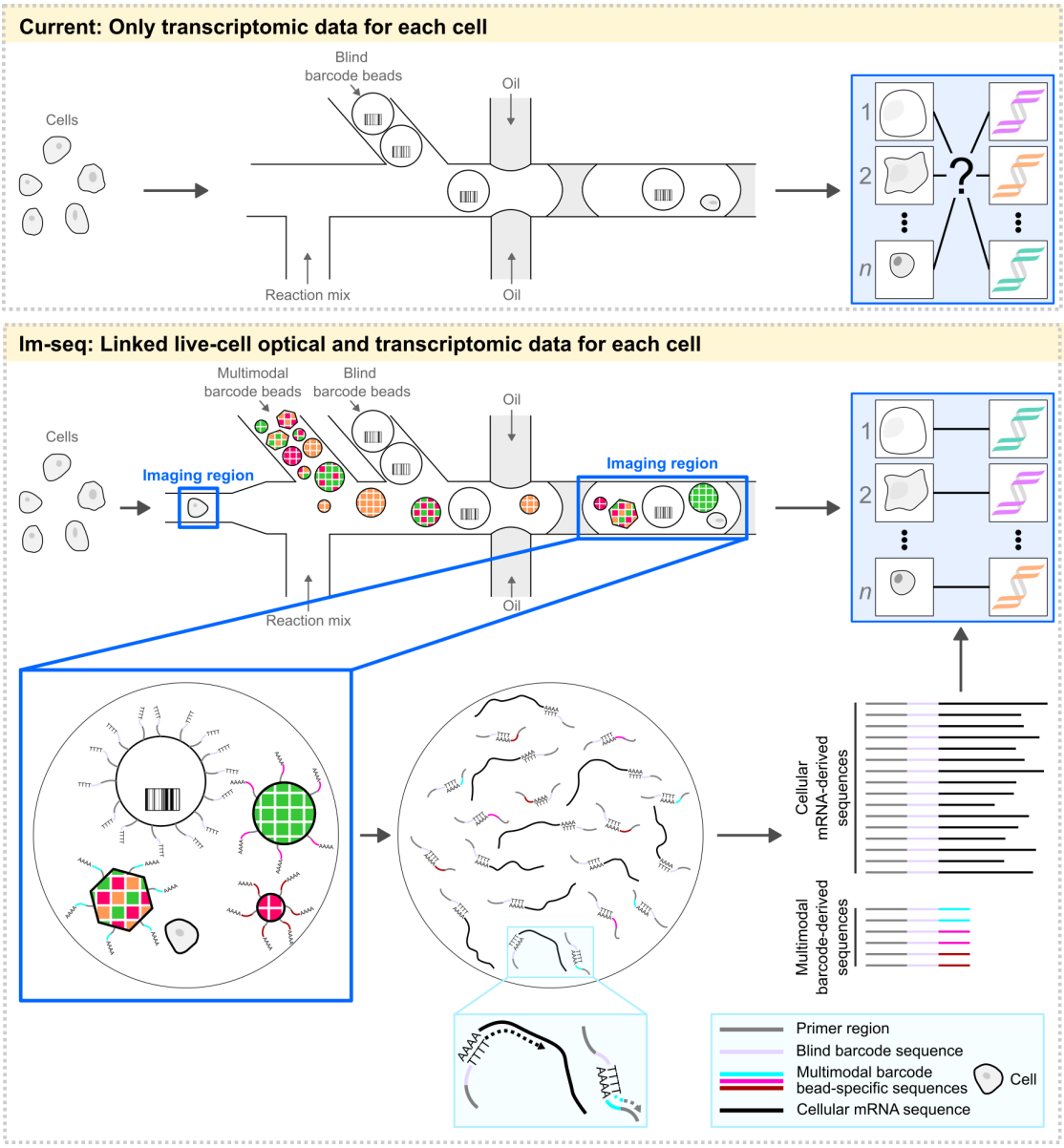

Figure 1: **Overview of im-seq.** Im-seq links together optical and gene expression data for live single cells in high throughput. In standard scRNA-seq, cells are encapsulated into droplets with barcode beads of unknown sequences ("blind barcode beads"). In im-seq, live cells are imaged immediately prior to encapsulation with both blind barcode beads and multimodal barcode beads. The multimodal barcode beads, which are functionalised with known DNA sequences, enable direct image-to-transcriptome linking of single cells.

These multimodal barcodes comprise multiple hydrogel beads, each carrying a unique sequence and known, unique optical signature [9, 21, 22]. By randomly combining multiple such beads together, we can construct immense numbers of multi-component barcodes; for example, 30 beads can yield over 1 billion unique combinations (Figure 2a). Identification of multimodal barcodes in droplets both optically and by sequencing thus directly links single-cell images to gene expression.

We synthesised unique hydrogel bead populations as barcode components by varying their size, shape, and colour [22, 23, 24] (Figure 2a-d), and reversibly conjugated each type to a unique, known DNA sequence. Component beads can be identified in droplets both optically and by sequencing, to yield the complete barcode (Figure 2b). In each droplet, the blind barcode bead tags all encapsulated nucleic acids: multimodal barcode DNA and cell mRNA, with the same unique sequence [25, 26]. The combinatorial multimodal barcode thereby links optical and sequencing data at the single-cell level.

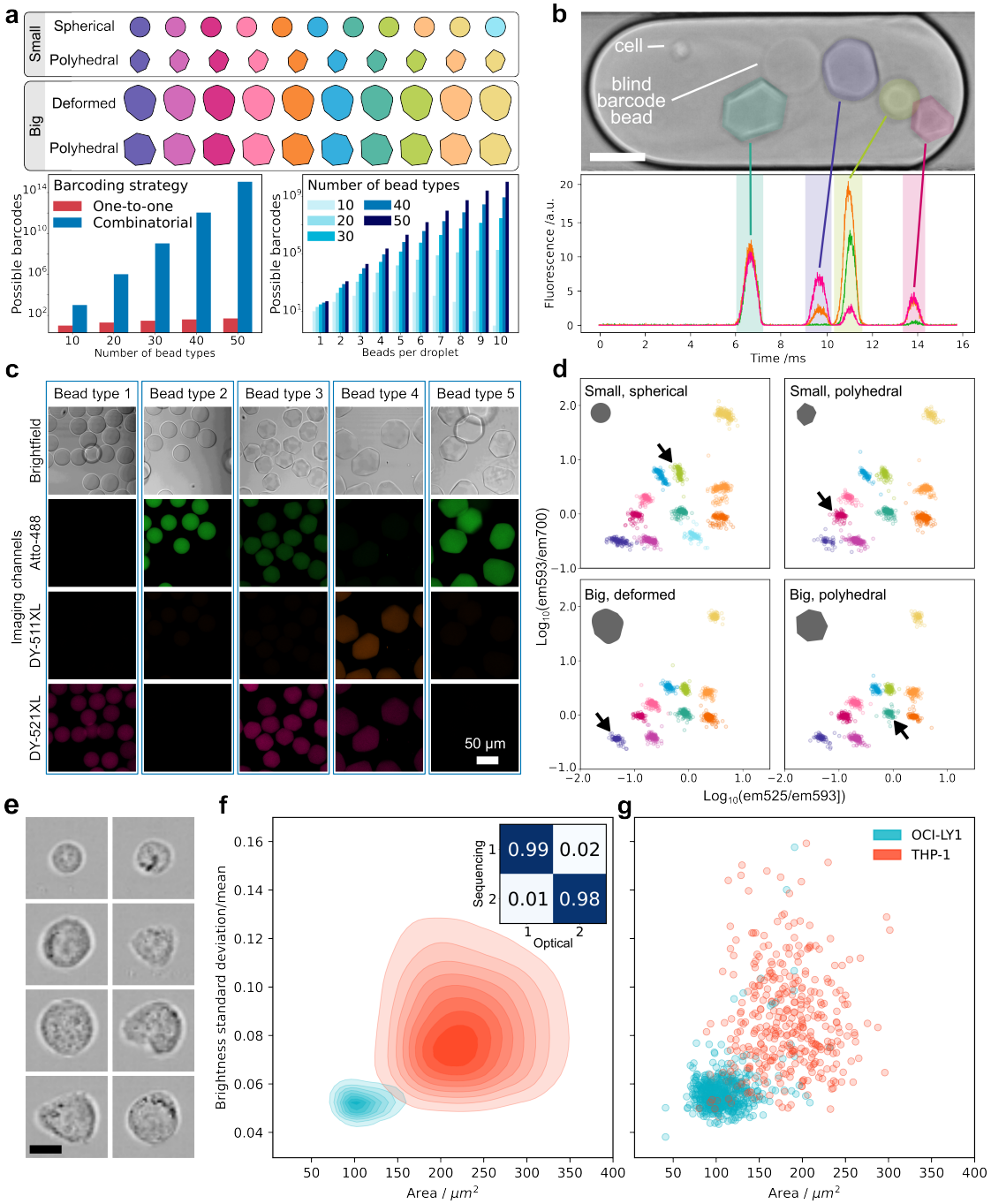
a
Small
Spherical
Polyhedral
Big
Deformed
Polyhedral
Barcoding strategy
One-to-one
Combinatorial
Possible barcodes
Number of bead types
Number of bead types
10
20
30
40
50
Beads per droplet
b
cell
blind barcode bead
Fluorescence /a.u.
Time /ms
c
Bead type 1
Bead type 2
Bead type 3
Bead type 4
Bead type 5
Brightfield
Imaging channels
Atto-488
DY-511XL
DY-521XL
50 µm
d
Small, spherical
Small, polyhedral
Big, deformed
Big, polyhedral
Log10(em593/em700)
Log10(em525/em593])
e
f
Brightness standard deviation/mean
Area / µm²
Sequencing
Optical
0.99
0.02
0.01
0.98
g
OCI-LY1
THP-1
Area / µm²

Figure 2: **Im-seq links single-cell image and gene expression.** (**a**) Multimodal barcode components can be produced by varying the size, shape and fluorescence colour of hydrogel beads. Huge numbers of multimodal barcodes can be generated by randomly combining components. (**b**) Droplet containing a cell, blind barcode bead, and four multimodal component beads which comprise the multimodal barcode. Fluorescence traces determine the colour of each bead (coloured as in (**d**)) (Scale bar: 50 µm.). (**c**) Example brightfield and fluorescence images of types (columns) of multimodal barcode beads. (**d**) Ratiometric bead colours defined by the combination of three fluorescent dyes. The three fluorescence signals (emission at 525, 593, and 700 nm) were reduced to two axes by taking the pairwise ratios, removing noise arising from variations in absolute fluorescence intensity. Colours are shown for the four size/shape combinations, with arrows indicating the bead types in the droplet in (**b**). (**e**) Example images of cells immediately prior to encapsulation in droplets. Scale bar: 10 µm. (**f**) Validation: OCI-LY1 (turquoise) and THP-1 (orange) imaged cells in separate measurements, showing distinct physical properties. Inset: ground truth validation of linking optical and sequencing data, by combining data from two separate experiments. In >98% of linked droplets, sequencing data were paired with optical droplet data from the same experiment class. (**g**) Plot of image features of 943 OCI-LY1 and THP-1 cells, coloured according to the gene expression-based cell type classification.

To validate that our multimodal barcodes are correctly and uniquely linked between imaging and sequencing data, we mixed data from two experiments. This produced one set of barcoded cell-containing droplets detected optically and another by sequencing, both originating from a mixture of experiment classes 1 and 2. We then analysed these mixed datasets to identify droplets with the same unique barcodes detected in both modalities. Comparison of these linked pairs with the known experiment classes confirmed that over 98% of matched droplets were correctly classified (Figure 2g (inset)), with mismatches likely originating from low signal-to-noise ratios in multimodal barcode bead sequencing for a minority of droplets. We next applied im-seq to a mixture of two cell lines: OCI-LY1 and THP-1, which differ in physical phenotype at the population level (Figure 2f), reproduced by cell type classification based on mRNA expression (Figure 2g). While

just two representative image-based parameters are displayed here, the dataset for each cell contains the whole image (Figure 2e).

We next explored gene expression–feature relationships in haematopoietic cell lines (HL-60, THP-1, and OCI-LY1). From the cell images, we extracted morphological parameters and interrogated associated transcriptional programmes, observing clearer separation between cell lines in gene-expression space than in image-feature space (Figure 3a, b) [27]. Annotating gene-expression embeddings with cellular imaging-derived properties demonstrated that detailed cell state descriptions require both imaging and gene expression data (Figure 3c, d).

Cell size differed substantially both across and within cell lines and thus serves as an easily interpretable showcase for linking image features to gene expression (Figure 3e). Correlation analyses across all cell lines identified both positively and negatively associated transcripts, including actin/cytoskeletal regulators such as CAP1 (positive) and TMSB4X (negative), as well as the cell-cycle inhibitor CDKN2A (negative) [28, 29]. Ribosomal genes were enriched among negatively correlated transcripts, consistent with cell-cycle–dependent regulation of translation, while immune and myeloid-state markers such as CHI3L1, ELANE, and LST1 were enriched among transcripts positively correlated with cell size (Figure 3f) [30, 31, 32, 33]. Closer inspection within cell lines revealed distinct classes of gene–image relationships, including genes whose apparent association is driven primarily by between–cell line differences versus genes that correlate consistently within each line; for example, the proliferation-associated TOP2A showed a positive association with cell size within, but not between, cell lines (Figure 3g-i).

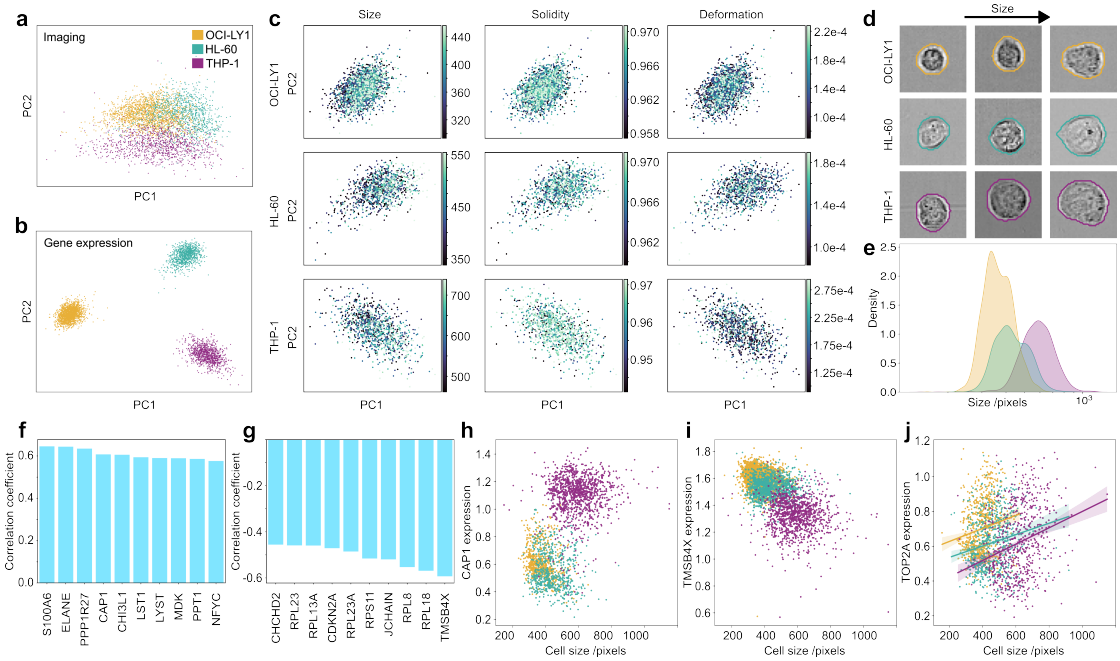

Figure 3: **Gene expression-imaging associations in haematopoietic cell lines** (**a**) Principal component analysis (PCA) of single-cell images of different cell lines acquired by im-seq. Images were featurised with CellProfiler [34]. Colours throughout the figure are yellow: OCI-LY1, turquoise: HL-60, and purple: THP-1. (**b**) PCA of single-cell gene expression in the same datasets as **a**). (**c**) PCA of single-cell gene expression for each cell line, coloured according to the magnitude of the indicated image-derived properties. (**d**) Example single-cell images of different cell lines, sorted according to cell size and shown alongside their segmentation. (**e**) Size distributions of cell lines as measured by im-seq. (**f** and **g**) Genes with the top ten most positively (**f**) and negatively (**g**) correlated expression with cell size across cell lines. (**h-j**) Examples of different types of correlations between cell size and the expression of individual genes observed by im-seq. Gene expression may be correlated across (**h**, **i**) or within (**j**) cell lines.

In conclusion, im-seq provides a general and scalable strategy for multimodal single-cell characterisation at high throughput, enabling live phenotype-gene expression studies not feasible under existing workflows. Approaches based on sorting cells into subpopulations discretise inherently continuous features and require that cell states of interest are pre-defined, limiting discovery of unexpected or multi-dimensional relationships. Current single-cell image-transcriptome linking

methods are limited in throughput and scalability due to the use of arrays or deterministic control. Our continuous flow-based approach is fast (currently 1000 cells in 5 minutes) and scalable. Moreover, the implementation is relatively simple, requiring only a commercially available microscope and syringe pumps, without complex liquid handling such as valves and controlled cell/droplet dispensing [12, 13, 11, 35].

The core concept of im-seq is modular and compatible with a broad range of cell characterisation modalities such as fluorescence imaging flow cytometry [36]. Moreover, since im-seq operates on live cells, it can be integrated with functional assays such as secretion profiling in droplets [15, 37] and perturbation screens [38, 39, 40], while also avoiding fixation-induced artefacts [14, 41]. We anticipate that im-seq will open new avenues for studying the relationship between cell phenotypes and gene expression programmes in health and disease.

Acknowledgements

We are grateful to Cornelia Liebers, Manuela Hauke, and Christine Schweitzer for culturing cells, to Dr Irina Harder, Parth Patel, and Dr Salvatore Girardo for their support in the clean room, and to Dr Arif Ekici and Dr Rinho Kim for their support with sequencing. We also thank Dr David Morse, Dr Tomasz Kaminski, and Professor Justus Kebschull for their helpful discussions. This research received funding from: the Peter und Traudl Engelhorn Stiftung fellowship (C.K.X), the HFSP Cross-Disciplinary Fellowship (C.K.X.), the Marie Skłodowska-Curie Actions fellowship READ-seq (agreement no. 101068803) (C.K.X.).

Author contributions

Project conception: C.K.X., G.M., J.G. Experiments: C.K.X., K.G. Software and analysis: C.K.X., G.M., N.M., N.S., M.F.S., T.P.J.K., F.T. Writing (original draft): C.K.X. Writing (reviewing and editing): C.K.X., G.M., N.S., N.M., K.G., A.S., M.F.S., T.P.J.K., F.T., L.M., J.G.

Competing interests

A patent has been filed for the technology (inventors C.K.X., G.M., T.P.J.K., and J.G) by the institutions Cambridge Enterprise and Max Planck Innovation (WO 2025/146377).

References

[1] Byungjin Hwang, Ji Hyun Lee, and Duhee Bang. Single-cell rna sequencing technologies and bioinformaticspipelines. *Experimental & Molecular Medicine*, 50(8):1–14, Aug 2018.

[2] Hayley M. Bennett, William Stephenson, Christopher M. Rose, and Spyros Darmanis. Single-cell proteomics enabled by next-generation sequencing or mass spectrometry. *Nature Methods*, 20(3):363–374, Mar 2023.

[3] Alev Baysoy, Zhiliang Bai, Rahul Satija, and Rong Fan. The technological landscape and applications of single-cell multi-omics. *Nature Reviews Molecular Cell Biology*, 24(10):695–713, Oct 2023.

[4] Camille L. G. Lambert, Guido van Mierlo, Johannes J. Bues, Orane J. Guillaume-Gentil, and Bart Deplancke. Engineering next-generation microfluidic technologies for single-cell phenomics. *Nature Genetics*, 57(6):1344–1356, Jun 2025.

[5] Jesse Q. Zhang, Christian A. Siltanen, Leqian Liu, Kai-Chun Chang, Zev J. Gartner, and Adam R. Abate. Linked optical and gene expression profiling of single cells at high-throughput. *Genome Biology*, 21(1):49, Feb 2020.

[6] Jinzhou Yuan, Jenny Sheng, and Peter A. Sims. Scope-seq: a scalable technology for linking live cell imaging and single-cell rna sequencing. *Genome Biology*, 19(1):227, Dec 2018.

[7] Zhouzerui Liu, Jinzhou Yuan, Anna Lasorella, Antonio Iavarone, Jeffrey N. Bruce, Peter Canoll, and Peter A. Sims. Integrating single-cell rna-seq and imaging with scope-seq2. *Scientific Reports*, 10(1):19482, Nov 2020.

[8] Fumiko Kawasaki, Yuka Mori, Takahiro Mimori, Issei Sato., and Sadao Ota. Identification of in-droplet multicellular communities by light-induced combinatorial dna barcoding. *Chemistry – A European Journal*, 29(53):e202301133, Sep 2023.

[9] Fumiko Kawasaki, Takahiro Mimori, Yuka Mori, Hiroyuki Aburatani, Nozomu Yachie, Issei Sato, and Sadao Ota. Computational design of synthetic optical barcodes in microdroplets. *Advanced Optical Materials*, 12(12):2302564, Apr 2024.

[10] Arata Tsuchida, Taikopaul Kaneko, Kaori Nishikawa, Mayu Kawasaki, Ryuji Yokokawa, and Hirofumi Shintaku. Opto-combinatorial indexing enables high-content transcriptomics by linking cell images and transcriptomes. *Lab on a Chip*, 24(8):2287–2297, 2024.

[11] Keara Lane, David Van Valen, Mialy M. DeFelice, Derek N. Macklin, Takamasa Kudo, Ariel Jaimovich, Ambrose Carr, Tobias Meyer, Dana Pe'er, Stéphane C. Boutet, and Markus W. Covert. Measuring signaling and rna-seq in the same cell links gene expression to dynamic patterns of nf-κb activation. *Cell Systems*, 4(4):458–469.e5, Apr 2017.

[12] Tyler N. Chen, Anushka Gupta, Mansi D. Zalavadia, and Aaron Streets. μcb-seq: microfluidic cell barcoding and sequencing for high-resolution imaging and sequencing of single cells. *Lab on a Chip*, 20(21):3899–3913, 2020.

[13] Johannes Bues, Joern Pezoldt, Camille Lucie Lambert, Benjamin David Hale, Elisa Bugani, Ramon Vinas Torne, Timothee Ferrari, Nadia Grenningloh, Vincent Gardeux, Shuo Wen, Caroline Wandinger, Maximilian Kohnen, Romina Augustin, Katharina Eckstein, Assia Ouanaya, Jillian Love, Sarthak Saha, Amirhossein Saba, Aviv Huttner, Maria Vittoria Impagliazzo, Jose Antonio Vasquez Porto Viso, Angel de Jesus Corria Osorio, Demetri Psaltis, Wouter Karthaus, Berend Snijder, Maria Brbic, and Bart Deplancke. Single-cell phenomics through integrated imaging and molecular profiling. *bioRxiv*, page 2025.11.28.690954, Jan 2025.

[14] Seong-Oh Kim, Joonhui Kim, Takaharu Okajima, and Nam-Joon Cho. Mechanical properties of paraformaldehyde-treated individual cells investigated by atomic force microscopy and scanning ion conductance microscopy. *Nano Convergence*, 4(1):5, Mar 2017.

[15] Klaus Eyer, Raphaël C. L. Doineau, Carlos E. Castrillon, Luis Briseño-Roa, Vera Menrath, Guillaume Mottet, Patrick England, Alexei Godina, Elodie Brient-Litzler, Clément Nizak, Allan Jensen, Andrew D. Griffiths, Jérôme Bibette, Pierre Bruhns, and Jean Baudry. Single-cell deep phenotyping of igg-secreting cells for high-resolution immune monitoring. *Nature Biotechnology*, 35(10):977–982, Oct 2017.

[16] Gunsagar S Gulati, Jeremy Philip D'Silva, Yunhe Liu, Linghua Wang, and Aaron M Newman. Profiling cell identity and tissue architecture with single-

cell and spatial transcriptomics. *Nat. Rev. Mol. Cell Biol.*, 26(1):11–31, January 2025.

[17] Charlotte Bunne, Yusuf Roohani, Yanay Rosen, Ankit Gupta, Xikun Zhang, Marcel Roed, Theo Alexandrov, Mohammed AlQuraishi, Patricia Brennan, Daniel B Burkhardt, Andrea Califano, Jonah Cool, Abby F Dernburg, Kirsty Ewing, Emily B Fox, Matthias Haury, Amy E Herr, Eric Horvitz, Patrick D Hsu, Viren Jain, Gregory R Johnson, Thomas Kalil, David R Kelley, Shana O Kelley, Anna Kreshuk, Tim Mitchison, Stephani Otte, Jay Shendure, Nicholas J Sofroniew, Fabian Theis, Christina V Theodoris, Srigokul Upadhyayula, Marc Valer, Bo Wang, Eric Xing, Serena Yeung-Levy, Marinka Zitnik, Theofanis Karaletsos, Aviv Regev, Emma Lundberg, Jure Leskovec, and Stephen R Quake. How to build the virtual cell with artificial intelligence: Priorities and opportunities. *Cell*, 187(25):7045–7063, December 2024.

[18] Allon M. Klein, Linas Mazutis, Ilke Akartuna, Naren Tallapragada, Adrian Veres, Victor Li, Leonid Peshkin, David A. Weitz, and Marc W. Kirschner. Droplet barcoding for single-cell transcriptomics applied to embryonic stem cells. *Cell*, 161(5):1187–1201, May 2015.

[19] Evan Z. Macosko, Anindita Basu, Rahul Satija, James Nemesh, Karthik Shekhar, Melissa Goldman, Itay Tirosh, Allison R. Bialas, Nolan Kamitaki, Emily M. Martersteck, John J. Trombetta, David A. Weitz, Joshua R. Sanes, Alex K. Shalek, Aviv Regev, and Steven A. McCarroll. Highly parallel genome-wide expression profiling of individual cells using nanoliter droplets. *Cell*, 161(5):1202–1214, May 2015.

[20] Rapolas Zilionis, Juozas Nainys, Adrian Veres, Virginia Savova, David Zemmour, Allon M. Klein, and Linas Mazutis. Single-cell barcoding and sequencing using droplet microfluidics. *Nature Protocols*, 12(1):44–73, Jan 2017.

[21] Paul H. Dannenberg, Jie Wang, Yue Zhuo, Sangyeon Cho, Kwon-Hyeon Kim, and Seok-Hyun Yun. Droplet microfluidic generation of a million optical microparticle barcodes. *Optics Express*, 29(23):38109–38118, Nov 2021.

[22] Yinnian Feng, Adam K. White, Jamin B. Hein, Eric A. Appel, and Polly M. Fordyce. Mrbles 2.0: High-throughput generation of chemically functionalized spectrally and magnetically encoded hydrogel beads using a simple single-layer microfluidic device. *Microsystems & Nanoengineering*, 6(1):109, Nov 2020.

[23] Daniel W. Weisgerber, Makiko Hatori, Xiangpeng Li, and Adam R. Abate. Polyhedral particles with controlled concavity by indentation templating. *Analytical Chemistry*, 94(21):7475–7482, May 2022.

[24] Sebastian Seiffert and Wilhelm Oppermann. Amine-functionalized polyacrylamide for labeling and crosslinking purposes. *Macromolecular Chemistry and Physics*, 208(16):1744–1752, Aug 2007.

[25] Marlon Stoeckius, Christoph Hafemeister, William Stephenson, Brian Houck-Loomis, Pratip K. Chattopadhyay, Harold Swerdlow, Rahul Satija, and Peter Smibert. Simultaneous epitope and transcriptome measurement in single cells. *Nature Methods*, 14(9):865–868, Sep 2017.

[26] Vanessa M. Peterson, Kelvin Xi Zhang, Namit Kumar, Jerelyn Wong, Lixia Li, Douglas C. Wilson, Renee Moore, Terrill K. McClanahan, Svetlana Sadekova, and Joel A. Klappenbach. Multiplexed quantification of proteins and transcripts in single cells. *Nature Biotechnology*, 35(10):936–939, Oct 2017.

[27] Sophia Clara Mädler, Niklas Arndt Schmacke, Alessandro Palma, Altana Namsaraeva, Ali Oğuz Can, Varvara Varlamova, Lukas Heumos, Mahima Arunkumar, Georg Wallmann, Veit Hornung, Fabian J Theis, and Matthias Mann. scportrait integrates single-cell images into multimodal modeling. September 2025.

[28] Enni Bertling, Pirta Hotulainen, Pieta K Mattila, Tanja Matilainen, Marjo Salminen, and Pekka Lappalainen. Cyclase-associated protein 1 (CAP1) promotes cofilin-induced actin dynamics in mammalian nonmuscle cells. *Mol. Biol. Cell*, 15(5):2324–2334, May 2004.

[29] C Simenel, M Van Troys, J Vandekerckhove, C Ampe, and M Delepierre. Structural requirements for thymosin beta4 in its contact with actin. an NMR-analysis of thymosin beta4 mutants in solution and correlation with their biological activity. *Eur. J. Biochem.*, 267(12):3530–3538, June 2000.

[30] Marvin E Tanenbaum, Noam Stern-Ginossar, Jonathan S Weissman, and Ronald D Vale. Regulation of mRNA translation during mitosis. *Elife*, 4:e07957, August 2015.

[31] Juanjuan Zhao, Quan Yuan, Haiyan Wang, Wei Liu, Xuejiao Liao, Yingying Su, Xin Wang, Jing Yuan, Tingdong Li, Jinxiu Li, Shen Qian, Congming

Hong, Fuxiang Wang, Yingxia Liu, Zhaoqin Wang, Qing He, Zhiyong Li, Bin He, Tianying Zhang, Yang Fu, Shengxiang Ge, Lei Liu, Jun Zhang, Ningshao Xia, and Zheng Zhang. Antibody responses to sars-cov-2 in patients with novel coronavirus disease 2019. *Clinical Infectious Diseases*, May 2020. ciaa344.

[32] Weilin Zeng, Yingqiu Song, Runze Wang, Rong He, and Tianlu Wang. Neutrophil elastase: From mechanisms to therapeutic potential. *J. Pharm. Anal.*, 13(4):355–366, April 2023.

[33] H Mulcahy, K P O'Rourke, C Adams, M G Molloy, and F O'Gara. LST1 and NCR3 expression in autoimmune inflammation and in response to IFN-gamma, LPS and microbial infection. *Immunogenetics*, 57(12):893–903, January 2006.

[34] Alán F Muñoz, Tim Treis, Alexandr A Kalinin, Shatavisha Dasgupta, Fabian Theis, Anne E Carpenter, and Shantanu Singh. cp_measure: API-first feature extraction for image-based profiling workflows. July 2025.

[35] Russell H. Cole, Shi-Yang Tang, Christian A. Siltanen, Payam Shahi, Jesse Q. Zhang, Sean Poust, Zev J. Gartner, and Adam R. Abate. Printed droplet microfluidics for on demand dispensing of picoliter droplets and cells. *Proceedings of the National Academy of Sciences*, 114(33):8728–8733, Aug 2017.

[36] Daniel Schraivogel, Terra M. Kuhn, Benedikt Rauscher, Marta Rodríguez-Martínez, Malte Paulsen, Keegan Owsley, Aaron Middlebrook, Christian Tischer, Beáta Ramasz, Diana Ordoñez-Rueda, Martina Dees, Sara Cuylen-Haering, Eric Diebold, and Lars M. Steinmetz. High-speed fluorescence image–enabled cell sorting. *Science*, 375(6578):315–320, Jan 2022.

[37] Annabelle Gérard, Adam Woolfe, Guillaume Mottet, Marcel Reichen, Carlos Castrillon, Vera Menrath, Sami Ellouze, Adeline Poitou, Raphaël Doineau, Luis Briseno-Roa, Pablo Canales-Herrerias, Pascaline Mary, Gregory Rose, Charina Ortega, Matthieu Delincé, Sosthene Essono, Bin Jia, Bruno Iannascoli, Odile Richard-Le Goff, Roshan Kumar, Samantha N. Stewart, Yannick Pousse, Bingqing Shen, Kevin Grosselin, Baptiste Saudemont, Antoine Sautel-Caillé, Alexei Godina, Scott McNamara, Klaus Eyer, Gaël A. Millot, Jean Baudry, Patrick England, Clément Nizak, Allan Jensen, Andrew D. Griffiths, Pierre Bruhns, and Colin Brenan. High-throughput single-cell activity-

based screening and sequencing of antibodies using droplet microfluidics. *Nature Biotechnology*, 38(6):715–721, Jun 2020.

[38] Atray Dixit, Oren Parnas, Biyu Li, Jenny Chen, Charles P. Fulco, Livnat Jerby-Arnon, Nemanja D. Marjanovic, Danielle Dionne, Tyler Burks, Raktima Raychowdhury, Britt Adamson, Thomas M. Norman, Eric S. Lander, Jonathan S. Weissman, Nir Friedman, and Aviv Regev. Perturb-seq: Dissecting molecular circuits with scalable single-cell rna profiling of pooled genetic screens. *Cell*, 167(7):1853–1866.e17, Dec 2016.

[39] Christoph Bock, Paul Datlinger, Florence Chardon, Matthew A Coelho, Matthew B Dong, Keith A Lawson, Tian Lu, Laetitia Maroc, Thomas M Norman, Bicna Song, Geoff Stanley, Sidi Chen, Mathew Garnett, Wei Li, Jason Moffat, Lei S Qi, Rebecca S Shapiro, Jay Shendure, Jonathan S Weissman, and Xiaowei Zhuang. High-content CRISPR screening. *Nat. Rev. Methods Primers*, 2(1):8, February 2022.

[40] Niklas A Schmacke, Sophia C Mädler, Georg Wallmann, Andreas Metousis, Marleen Bérouti, Hartmann Harz, Heinrich Leonhardt, Matthias Mann, and Veit Hornung. SPARCS, a platform for genome-scale CRISPR screening for spatial cellular phenotypes. June 2023.

[41] Leah C Wehmas, Susan D Hester, and Charles E Wood. Direct formalin fixation induces widespread transcriptomic effects in archival tissue samples. *Sci. Rep.*, 10(1):14497, September 2020.